Reduced technique for modeling electromagnetic immunity on braid shielding cable bundles*

Pei Xiao(肖培), Ping-An Du(杜平安)†, Bao-Lin Nie(聂宝林), and Dan Ren(任丹)

Department of Mechatronics Engineering, University of Electronic Science and Technology of China, Chengdu 611731, *China*

(Received 17 February 2017; revised manuscript received 31 March 2017; published online 27 July 2017)

In this paper, an efficient multi-conductor simplification technique is proposed to model the electromagnetic immunity on cable bundles within a braid shielding structure over a large frequency range. By grouping together the conductors based on the knowledge of *Z*-Smith chart, the required computation time is markedly reduced and the complexity of modeling the completely shielding cable bundles is significantly simplified with a good accuracy. After a brief description of the immunity problems in shielding structure, a six-phase procedure is detailed to generate the geometrical characteristics of the reduced cable bundles. Numerical simulation is carried out by using a commercial software CST to validate the efficiency and advantages of the proposed approach. The research addressed in this paper is considered as a simplified modeling technique for the electromagnetic immunity within a shielding structure.

Keywords: cable bundles, electromagnetic immunity, braid shielding structure, numerical simulation

PACS: 41.20.–q, 41.20.Jb, 41.90.+e **DOI:** 10.1088/1674-1056/26/9/094102

1. Introduction

In modern industrial domains such as the automotive industry and aviation industry, reliably and efficiently generating a full numerical model of complex real systems has become a difficult task for the designers.[1,2] Numerical modeling method and simulation have been widely used in the electromagnetic compatibility (EMC) analysis.[3–5] It requires a reliable model of the target electrical structure, in particular the model of the cable harness.[6,7] In order to simplify the structural modeling and improve the analytic efficiency, this paper focuses on the reduction technique of braid shielding cable bundles.

The electromagnetic (EM) coupling mechanism on cable harnesses in a real system has been widely studied based on the theory of multiconductor transmission line networks (MTLN).[8–13] Compared with numerical simulation in calculating EM fields, the MTLN formalism performs better accuracy and needs less computation time. Unfortunately, the MTLN model behaves inefficiently at high frequencies due to the appearance of nonquasi-TEM modes. Hence, many researchers put forward hybrid methods to handle the EM coupling situations on cable harnesses.[14,15] In addition, some researchers adopted measurement approaches to deal with their modeling.[16] However, despite the rapid improvement in computer performance, it is still impossible to perform an accurate computation on the complete model of the whole realistic cable harnesses.

Previous work on elaborating an EMC model for the cable harness with so called "equivalent cable bundle method (ECBM)" has been reported. On the assumption that the common-mode (CM) response is more critical than the differential-mode response for the EM coupling problems, the ECBM for modeling CM currents on cable bundles at high frequency for automotive applications is proposed for the first time.[17] Then, this technique is extended to model EM emissions of complex cable bundles.[18] Recently, the ECBM has been adopted to model the crosstalk of complex cable bundles[19,20] and calculate the conducted rear-door disturbances at a vehicle level with a huge number of wires.[21,22]

In this paper, an efficient reduced technique is proposed to handle the modeling of the EM immunity prediction of complex cable bundles within a braid shielding structure. For this new kind of application, the main assumption is the same as that addressed in Ref. [17]. The rest of this paper is organized as follows. Section 2 presents the equivalent process of the simplification technique in detail, which contains conductor grouping and equivalent geometrical characteristics. In Section 3, we validate the proposed method with a model of braid shielding 14-conductors by using CST Cable Studio and the FSV technique is used to analyze the comparison between the results from the complete model and those from the reduced model. Finally, some comments on the proposed simplification technique are given in Section 4.

2. Theory

2.1. Immunity problems on shielding cable bundles

Figure 1 illustrates a model of n-conductor bounded in a braid shielding structure and irradiated by an incident EM field. The radiation field excites the induced current along each conductor. For the immunity problems, the huge com-

*Project supported by the National Natural Science Foundation of China (Grant No. 51675086) and the National Defense Pre-Research Foundation of China (Grant No. 6140758010116DZ02002).

†Corresponding author. E-mail: dupingan@uestc.edu.cn

© 2017 Chinese Physical Society and IOP Publishing Ltd

plexity of the whole cable bundles seems to be unreasonable to model when considering the required computer resources. Though previous "ECBM" puts forward a solution to the immunity case that all the equivalent unshielded conductors are located above the infinite ideal conducting plane, it cannot be directly used to simplify the modeling of the coupling prediction of the conductors within the shielding screen. Thus, this paper focuses on a multiconductor reduction technique for modeling immunity problem on shielding cable bundles. The presented technique overcomes the limit to the MTL formalism at high frequency by using three-dimensional (3D) computation codes.

The generation of the equivalent cross-section geometrical characteristic parameters in the braid shielding structure is quite different from that in the half-free space. As the analytical expressions of self and mutual inductance of the braid shielding multiconductors are difficult to obtain, an approximate model of multiconductors within an ideal conducting cylindrical shield is adopted to compute the electrical parameters. In this paper, we define a central distance d and central angle θ to determine the relative position parameters of the reduced bundles. It should be noted that the shield transfer impedance associated with inductance is not discussed in the simplification technique because the approximate method is used in computing the inductance of braid shielding multiconductors. We do not need to analyze the coupling mechanism by using the shield transfer impedance, because it is considered in the CST simulation.

The purpose of the approach is to lower the computation time and simplify the modeling process by reducing the multiconductor cable bundles model into four groups shown in Fig. 2. For the immunity problems, the provided modeling technique presents a modified six-phase procedure to generate the electrical and geometrical characteristic parameters of the reduced cable bundles, which contains conductor grouping, cable bundle matrices reduction, cross-section geometry modeling and equivalent loads determination. The creation of groups of conductors is based on the knowledge of Z-Smith chart, which provides a convenient way to describe the relationship between load impedance and reflection coefficient. The whole problem is calculated over a large frequency range. Based on the assumption in Ref. [17], the proposed simplification technique provides a way of modeling the CM current induced at the extremity of inner conductors.

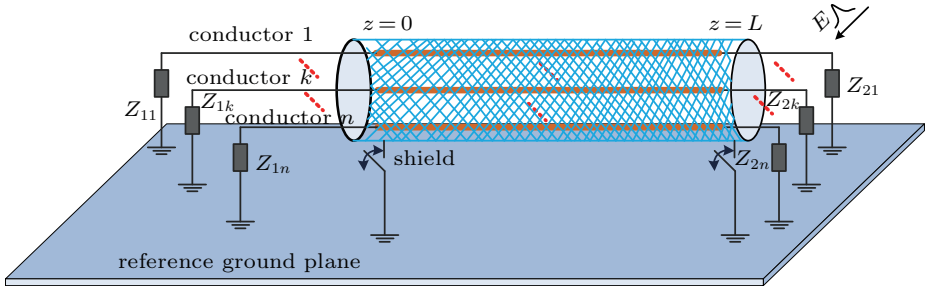


Fig. 1. (color online) Illustration of the electromagnetic immunity on braid shielding multiconductor cable bundles model.

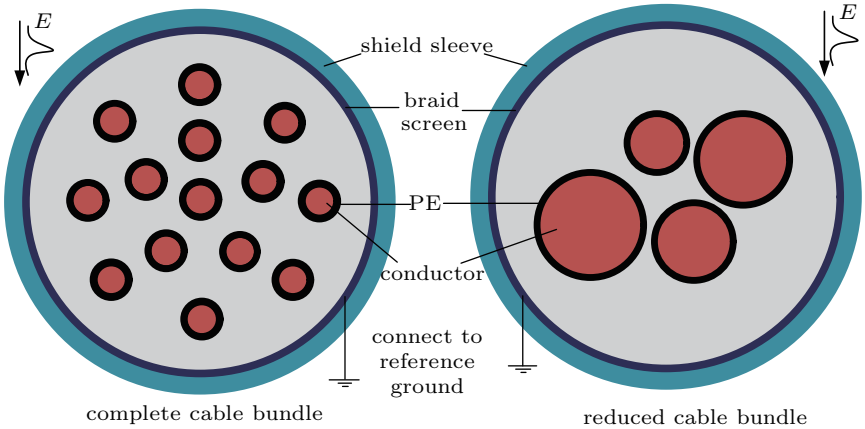


Fig. 2. (color online) Cross-section geometries of the complete and reduced cable bundle.

2.2. Presentation of the procedure

a) Step 1: Creation of groups of conductors based on Z-Smith chart

In the first step, all the conductors of the complete cable bundle are classified as four groups with respect to the location of normalized terminal load $|Z_{ij}|$ in Z-Smith chart, where $|Z_{ij}| = Z_{ij}^{\mathrm{L}}/Z_{\mathrm{C}}$, Z_{ij}^{L} represents the terminal impedance and Z_{C} the equivalent CM characteristic impedance of all conductors,

i corresponds to the terminal number ("1" represents the near end terminal and "2" the far end terminal) and j the conductor number as illustrated in Table 1. It should be noted that the management of the cable harness grouping is just to simplify the coupling CM current calculation and the classification method will not affect the overall performance.

Table 1. Conductor classification table.

	Extremity 1	Extremity 2
Group 1	$Z_{1j} \in \mathrm{I}_1$	$Z_{2j} \in \mathrm{II}_1$
Group 2	$Z_{1j} \in \mathrm{I}_1$	$Z_{2j} \in \mathrm{II}_2$
Group 3	$Z_{1j} \in \mathrm{I}_2$	$Z_{2j} \in \mathrm{II}_1$
Group 4	$Z_{1j} \in \mathrm{I}_2$	$Z_{2j} \in \mathrm{II}_2$

Figure 3 demonstrates the classification of groups of 9-conductor model. The dots in the Z-Smith chart represent near end normalized loads of each conductor, while the asterisks represent far end normalized loads. All the dots and asterisks are included in four sections denoted by I_1, I_2, II_1, and II_2. From the characteristic of Z-Smith chart, the terminal load has similar reflective properties in an adjacent area. Here, let $\left|Z_{1m}^{\mathrm{L}}/Z_{\mathrm{C}}\right| < 1$, $\left|Z_{1n}^{\mathrm{L}}/Z_{\mathrm{C}}\right| < 1$, where Z_{1m}^{L} and Z_{1n}^{L} are the arbitrary terminal impedances connected to the near ends. Then we can obtain the following inequality:

$$f = \mathrm{Abs}\left(\left|\frac{Z_{1m}^{\mathrm{L}}}{Z_{\mathrm{C}}}\right| - \left|\frac{Z_{1n}^{\mathrm{L}}}{Z_{\mathrm{C}}}\right|\right) < \left|\frac{Z_{1m}^{\mathrm{L}} - Z_{1n}^{\mathrm{L}}}{Z_{\mathrm{C}}}\right| < 1, \tag{1}$$

where f is described as the distance between arbitrary Z_{1m}^{L} and Z_{1n}^{L}. The criterion of cable bundle grouping can be established by f. Then, we define I_1 as the area of $f < 1$ with a set of a maximum number points on the graph which satisfy the condition, which means the absolute distance value of the two arbitrary normalized near end terminal loads is less than 1. Then I_2 the rest normalized near end loads. The II_1 and II_2 can be defined in the same manner, which means $f < 1$ in II_1 and the rest in II_2. Thus the 9 conductors can be sorted into 4 groups.

b) Step 2: Reduced cable bundle matrices

The second step aims to determine the reduced cable bundle inductance $[L_{\mathrm{eq}}]$ and capacitance matrix $[C_{\mathrm{eq}}]$. According to the general MTLN theory, the equations of N-conductor cable bundle can be written as

$$\frac{\partial}{\partial z}[V]_{N\times 1} = -\mathrm{j}\omega\,[L]_{N\times N}\,[I]_{N\times 1}, \tag{2}$$

$$\frac{\partial}{\partial z}[I]_{N\times 1} = -\mathrm{j}\omega\,[C]_{N\times N}\,[V]_{N\times 1}. \tag{3}$$

On the assumption that the same group CM current I_{gci} equals the sum of the currents induced on each conductor of the group and all the conductors in group i have the same group voltage V_{gci}, the reduced cable bundle containing four conductors is established and the equivalent MTLN equations can be modified as

$$\frac{\partial}{\partial z}\left[V_{\mathrm{gci}}\right]_{4\times 1} = -\mathrm{j}\omega\left[L_{\mathrm{eq}}\right]_{4\times 4}\left[I_{\mathrm{gci}}\right]_{4\times 1}, \tag{4}$$

$$\frac{\partial}{\partial z}\left[I_{\mathrm{gci}}\right]_{4\times 1} = -\mathrm{j}\omega\left[C_{\mathrm{eq}}\right]_{4\times 4}\left[V_{\mathrm{gci}}\right]_{4\times 1}. \tag{5}$$

From Eqs. (1)–(4), the reduced inductance matrix $[L_{\mathrm{eq}}]$ and capacitance matrix $[C_{\mathrm{eq}}]$ can be obtained as follows:[23]

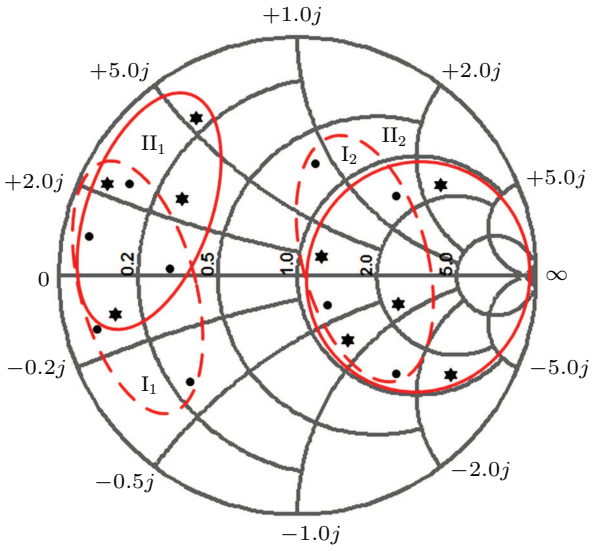


Fig. 3. (color online) Criterion of cable bundle grouping based on the Z-Smith chart.

$$[L_{\mathrm{eq}}] = \begin{bmatrix} \frac{\sum_{p=1}^{\alpha}\sum_{q=1}^{\alpha} L_{pq}}{N_1^2} & \frac{\sum_{p=1}^{\alpha}\sum_{q=\alpha+1}^{\beta} L_{pq}}{N_1N_2} & \frac{\sum_{p=1}^{\alpha}\sum_{q=\beta+1}^{\xi} L_{pq}}{N_1N_3} & \frac{\sum_{p=1}^{\alpha}\sum_{q=\xi+1}^{N} L_{pq}}{N_1N_4} \\ \frac{\sum_{p=\alpha+1}^{\beta}\sum_{q=1}^{\alpha} L_{pq}}{N_1N_2} & \frac{\sum_{p=\alpha+1}^{\beta}\sum_{q=\alpha+1}^{\beta} L_{pq}}{N_2^2} & \frac{\sum_{p=\alpha+1}^{\beta}\sum_{q=\beta+1}^{\xi} L_{pq}}{N_2N_3} & \frac{\sum_{p=\alpha+1}^{\beta}\sum_{q=\xi+1}^{N} L_{pq}}{N_2N_4} \\ \frac{\sum_{p=\beta+1}^{\xi}\sum_{q=1}^{\alpha} L_{pq}}{N_1N_3} & \frac{\sum_{p=\beta+1}^{\xi}\sum_{q=\alpha+1}^{\beta} L_{pq}}{N_2N_3} & \frac{\sum_{p=\beta+1}^{\xi}\sum_{q=\beta+1}^{\xi} L_{pq}}{N_3^2} & \frac{\sum_{p=\beta+1}^{\xi}\sum_{q=\xi+1}^{N} L_{pq}}{N_3N_4} \\ \frac{\sum_{p=\xi+1}^{N}\sum_{q=1}^{\alpha} L_{pq}}{N_1N_4} & \frac{\sum_{p=\xi+1}^{N}\sum_{q=\alpha+1}^{\beta} L_{pq}}{N_2N_4} & \frac{\sum_{p=\xi+1}^{N}\sum_{q=\beta+1}^{\xi} L_{pq}}{N_3N_4} & \frac{\sum_{p=\xi+1}^{N}\sum_{q=\xi+1}^{N} L_{pq}}{N_4^2} \end{bmatrix}, \tag{6}$$

$$[C_{\rm eq}] = \begin{bmatrix} \sum_{p=1}^{\alpha}\sum_{q=1}^{\alpha} C_{pq} & \sum_{p=1}^{\alpha}\sum_{q=\alpha+1}^{\beta} C_{pq} & \sum_{p=1}^{\alpha}\sum_{q=\beta+1}^{\xi} C_{pq} & \sum_{p=1}^{\alpha}\sum_{q=\xi+1}^{N} C_{pq} \\ \sum_{p=\alpha+1}^{\beta}\sum_{q=1}^{\alpha} C_{pq} & \sum_{p=\alpha+1}^{\beta}\sum_{q=\alpha+1}^{\beta} C_{pq} & \sum_{p=\alpha+1}^{\beta}\sum_{q=\beta+1}^{\xi} C_{pq} & \sum_{p=\alpha+1}^{\beta}\sum_{q=\xi+1}^{N} C_{pq} \\ \sum_{p=\beta+1}^{\xi}\sum_{q=1}^{\alpha} C_{pq} & \sum_{p=\beta+1}^{\xi}\sum_{q=\alpha+1}^{\beta} C_{pq} & \sum_{p=\beta+1}^{\xi}\sum_{q=\beta+1}^{\xi} C_{pq} & \sum_{p=\beta+1}^{\xi}\sum_{q=\xi+1}^{N} C_{pq} \\ \sum_{p=\xi+1}^{N}\sum_{q=1}^{\alpha} C_{pq} & \sum_{p=\xi+1}^{N}\sum_{q=\alpha+1}^{\beta} C_{pq} & \sum_{p=\xi+1}^{N}\sum_{q=\beta+1}^{\xi} C_{pq} & \sum_{p=\xi+1}^{N}\sum_{q=\xi+1}^{N} C_{pq} \end{bmatrix}, \tag{7}$$

where group 1 contains conductor $1-\alpha$ with the total number N_1, group 2 conductor $(\alpha+1)-\beta$ with the total number N_2, group 3 conductor $(\beta+1)-\xi$ with the total number N_3, group 4 conductor $(\xi+1)-N$ with the total number N_4.

c) Step 3: Reduced cable bundle cross-section geometry

The third step is to generate the cross-section of the reduced cable bundle, which consists of six phases. As the inductance parameters of the shielding multiconductor are associated with the structural factors, such as the distance between the analytical conductor and screen, the relative distance among conductors, the calculation of the cross-sectional geometry parameters of equivalent model are obtained thanks to study made in Ref. [24] and the knowledge of the $[L_{\rm eq}]$ and $[C_{\rm eq}]$ matrices.

1) Phase 1: Estimate the central distance d_i between each equivalent conductor and the central axis of the braid shielding structure. Distance d_i of each equivalent conductor corresponds to the average of the distance of all the conductors of the group.

2) Phase 2: Estimate the radius r_i of the braid shielding structure. The analytical formula for self-inductance l_{ii} of a wire in an ideal perfectly conducting shield is equal to $l_{ii} = (\mu/2\pi)\mathrm{In}[(r_{\rm s}^2 - d_i^2)/r_{\rm s}r_i]$. Thus, the radius r_i of each equivalent conductor can be approximated by

$$r_i = \frac{r_{\rm s}^2 - d_i^2}{r_{\rm s}\exp\left(\dfrac{2\pi l_{ii}}{\mu}\right)}. \tag{8}$$

3) Phase 3: The analytical formula of mutual inductance l_{ij} between two conductors in an ideal perfectly conducting shield can be written as

$$l_{ij} = \frac{\mu}{2\pi}\mathrm{In}\left(\frac{d_j}{r_{\rm s}}\sqrt{\frac{(d_i d_j)^2 + r_{\rm s}^4 - 2d_i d_j r_{\rm s}^2\cos\theta_{ij}}{(d_i d_j)^2 + d_j^4 - 2d_i d_j^3\cos\theta_{ij}}}\right). \tag{9}$$

Thus, the central angle between two conductors can be approximated by

$$\theta_{ij} = \arccos\frac{M\left((d_i d_j)^2 + d_j^4\right) - \left((d_i d_j)^2 + r_{\rm s}^4\right)}{2Md_i d_j^3 - 2d_i d_j r_{\rm s}^2}, \tag{10}$$

where

$$M = \left(\frac{r_{\rm s}}{d_j}\exp\left(\frac{2\pi l_{ij}}{\mu}\right)\right)^2.$$

4) Phase 4: Optimize the reduced cross-section geometrical parameter d_i, r_i, and θ_{ij} based on the dichotomic optimization and exact electrostatic calculations.

5) Phase 5: Determine the thickness of the dielectric coating surrounding each equivalent conductor while avoiding dielectric coating overlapping.

6) Phase 6: Calculate and optimize the relative permittivity $\varepsilon_{\rm r}$ of each wire dielectric coating, which is in accordance with the $[C_{\rm eq}]$ matrix using an electrostatic calculation.

Figure 4 shows the corresponding computational process of the proposed simplification technique used to build the cross-section geometry. Computational process for modeling the cross-section geometry of a reduced cable bundle in braid shielding structure.

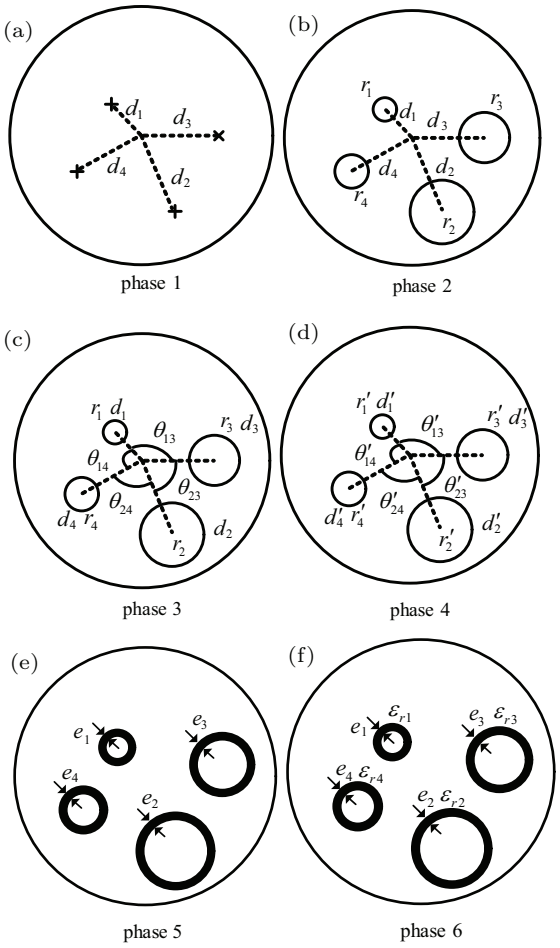


Fig. 4. Computational process for modeling the cross-section geometry of a reduced cable bundle in braid shielding structure. (a)–(f) Phases 1–6.

d) Step 4: Reduced cable bundle equivalent terminal loads

The fourth and the last step consists in computing the terminal loads of the reduced model connected to each equivalent conductor end. Here, the equivalent CM loads are defined as the loads that connect conductor ends to the shield screen. The terminal load connected to an equivalent conductor end is equal to the loads at the same end of all the conductors of the group connected in parallel.

It should be noted that the previous four-step procedure is used for a simple point-to-point connected shielding cable bundle. Nevertheless, due to the calculation methods of the self and mutual inductance of shielding multiconductor, there are two important restrictions on their applicability. These are that the wires must be widely separated and the dielectric medium surrounding the wires must be homogeneous. The charge distributions around closely spaced wires will be nonuniform around their peripheries but will be approximately uniform for ratios of wire separation to wire-radius 4 and higher.

3. Validations of reduction technique by numerical models

In this section, a model of braid shielding 14-conductor is constructed to validate the proposed reduced technique with a commercial tool CST. Please note that in the following simulations the number of the same group conductors is chosen arbitrarily in order to demonstrate the universality of the presented approach to immunity prediction problems.

3.1. Complete and reduced braid shielding cable bundle description

As illustrated in Fig. 2, a 14-conductor point-to-point connected cable bundle, 1-meter long, located in a copper braid shielding structure with a radius of 12 mm and a thickness of 0.5 mm is modeled. Each conductor has a radius of 0.5 mm and is surrounded by dielectric coating with a thickness of 0.2 mm and dielectric constant of $\varepsilon_r = 2.5$ and $\mu_r = 1$. The conductors with a serial number "2, 3, 4, 5, 6" are evenly distributed on the circle with a radius of 2 mm, while the conductors with a serial number "6, 7, 8, 9, 10, 11, 12, 13, 14" on the circle with a radius of 4 mm. The central coordinate of each conductor is presented in Table 2. By using modal analysis,[19] the analytical 14-conductor cable bundle characteristic impedance Z_C equals 244.4 Ω. The terminal loads connected to the ends of each conductor are described in Table 3. According to the classification method proposed in the first equivalent step, the 14-conductor can be sorted into the following four groups:

1) group 1: conductors 1, 2, 12;

2) group 2: conductors 3, 6, 14;

3) group 3: conductors 4, 5, 7, 8;

4) group 4: conductors 9, 10, 11, 13.

The p.u.l. inductance matrix [L] and capacitance matrix [C] of the complete model in Fig. 5 are

$$L = \begin{bmatrix} 555.8 & 312.0 & 312.3 & 311.7 & 311.7 & 312.3 & 210.4 & 207.3 & 208.5 & 209.7 & 206.8 & 209.8 & 208.5 & 207.3 \\ & 566.3 & 286.9 & 221.0 & 220.9 & 286.9 & 315.1 & 248.1 & 191.3 & 161.5 & 151.7 & 161.5 & 191.3 & 248.1 \\ & & 566.9 & 286.7 & 221.0 & 221.5 & 210.8 & 282.1 & 298.4 & 221.3 & 175.3 & 156.3 & 154.1 & 169.4 \\ & & & 566.6 & 286.0 & 221.0 & 158.7 & 182.6 & 233.9 & 310.9 & 264.7 & 200.4 & 164.7 & 152.2 \\ & & & & 566.6 & 286.7 & 158.7 & 152.2 & 164.7 & 200.4 & 264.7 & 310.9 & 233.9 & 182.6 \\ & & & & & 566.9 & 210.8 & 169.4 & 154.1 & 156.3 & 175.3 & 221.3 & 298.4 & 282.1 \\ & & & & & & 576.7 & 239.8 & 153.0 & 120.2 & 110.9 & 120.2 & 153.0 & 239.8 \\ & & & & & & & 580.1 & 241.1 & 152.2 & 119.0 & 110.8 & 119.4 & 151.4 \\ & & & & & & & & 578.8 & 239.2 & 151.7 & 119.8 & 110.8 & 119.4 \\ & & & & & & & & & 577.3 & 240.5 & 153.3 & 119.8 & 110.8 \\ & & & & & & & & & & 580.6 & 240.5 & 151.7 & 119.0 \\ & & & & & & & & & & & 577.33 & 239.2 & 152.2 \\ & & & & & & & & & & & & 578.8 & 241.1 \\ & & & & & & & & & & & & & 580.1 \end{bmatrix}, \quad (11)$$

Table 2. Coordinates of each conductor of the 14-conductor shielding cable bundle (unit: mm).

Conductor	1	2	3	4	5	6	7
(x, y)	(0,0)	(0,2)	(1.9,0.62)	(1.18, −1.62)	(−1.18, −1.62)	(−1.9,0.62)	(0,4)
Conductor	8	9	10	11	12	13	14
(x, y)	(2.83,2.83)	(4,0)	(2.83, −2.83)	(0, −4)	(−2.83, −2.83)	(−4,0)	(−2.83, 2.83)

Table 3. Terminal loads of the 14-conductor shielding cable bundle.

Conductor	1	2	3	4	5	6	7
Near end Z_1(Ω, nH, pF)	(50, 10, 0)	(100, 5, 0)	(1.0×10^4, 0, 0.5)	(50, 0, 0)	(20, 0, 0)	(5.0×10^3, 0, 0.2)	(100, 0, 0)
Far end Z_2(Ω, nH, pF)	(10, 0, 100)	(60, 0, 50)	(1.0×10^3, 500, 0)	(1.0×10^3, 0, 0)	(2.0×10^3, 0, 0)	(1.5×10^4, 2.0×10^3, 0)	(1.0×10^4, 400, 0)
Conductor	8	9	10	11	12	13	14
Near end Z_1(Ω, nH, pF)	(15, 0, 0)	(1.0×10^6, 0, 0.01)	(1.0×10^4, 0, 0.1)	(1.0×10^3, 300, 0)	(80, 6, 0)	(1.5×10^4, 1.0×10^3, 0)	(5.0×10^3, 0, 0)
Far end Z_2(Ω, nH, pF)	(3.0×10^3, 0, 0)	(50, 1, 0)	(20, 3, 0)	(100, 0, 100)	(40, 10, 0)	(15, 0, 50)	(8.0×10^3, 1.0×10^3, 0)

$$C = \begin{bmatrix} 45.03 & -8.66 & -8.67 & -8.64 & -8.64 & -8.67 & -0.15 & -0.25 & -0.22 & -0.17 & -0.28 & -0.17 & -0.22 & -0.25 \\ & 40.17 & -5.89 & -0.10 & -0.10 & -5.89 & -11.25 & -3.72 & -0.15 & -0.01 & -0.002 & -0.01 & -0.15 & -3.72 \\ & & 39.84 & -5.87 & -0.10 & -0.10 & -0.68 & -7.38 & -9.22 & -1.31 & -0.04 & -0.004 & -0.002 & -0.03 \\ & & & 40.01 & -5.82 & -0.10 & -0.006 & -0.07 & -2.34 & -10.72 & -5.47 & -0.33 & -0.02 & -0.002 \\ & & & & 40.01 & -5.87 & -0.006 & -0.002 & -0.02 & -0.33 & -5.47 & -10.72 & -2.34 & -0.07 \\ & & & & & 39.84 & -0.69 & -0.03 & -0.002 & -0.004 & -0.04 & -1.31 & -9.22 & -7.38 \\ & & & & & & 30.97 & -5.74 & -0.24 & -0.02 & -0.004 & -0.02 & -0.24 & -5.75 \\ & & & & & & & 29.29 & -5.38 & -0.24 & -0.02 & -0.004 & -0.02 & -0.24 \\ & & & & & & & & 29.95 & -5.91 & -0.24 & -0.02 & -0.004 & -0.02 \\ & & & & & & & & & 30.68 & -5.51 & -0.24 & -0.02 & -0.004 \\ & & & & & & & & & & 29.04 & -5.52 & -0.24 & -0.02 \\ & & & & & & & & & & & 30.68 & -5.91 & -0.24 \\ & & & & & & & & & & & & 29.94 & -5.37 \\ & & & & & & & & & & & & & 29.29 \end{bmatrix}. \quad (12)$$

Hereafter, inserting Eqs. (11) and (12) into Eqs. (6) and (7), the reduced p.u.l. inductance matrix $[L_{\rm eq}]$ and capacitance matrix $[C_{\rm eq}]$ can be written as follows:

$$[L_{\rm eq}] = \begin{bmatrix} 390.2 & 266.0 & 230.4 & 186.7 \\ & 365.3 & 187.7 & 229.3 \\ & & 287.7 & 140.7 \\ & & & 287.7 \end{bmatrix}, \quad (13)$$

$$[C_{\rm eq}] = \begin{bmatrix} 8.73 & -4.24 & -2.88 & -0.41 \\ & 10.69 & -1.18 & -3.53 \\ & & 5.36 & -0.77 \\ & & & 5.27 \end{bmatrix}. \quad (14)$$

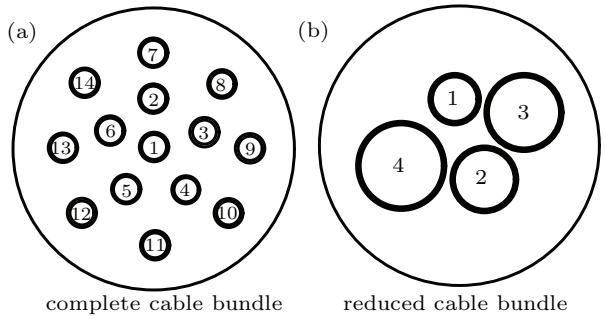


Fig. 5. (a) Cross-sectional geometry of the 14-conductor complete shielding cable bundle model and (b) the corresponding 4-equivalent-conductor reduced shielding cable bundle model.

After applying the six-phase procedure described in the third step in Section 2, the cross-section geometry of 4-equivalent-conductor model is obtained and illustrated in Fig. 5. The equivalent CM terminal loads are calculated and the results are listed in Table 4. In addition, the relevant central distance, radius and central coordinate are listed in Table 5.

Cross-sectional geometry of the 14-conductor complete shielding cable bundle model and the corresponding 4-equivalent-conductor reduced shielding cable bundle model.

Table 4. Terminal loads of each conductor of the reduced shielding bundle.

Conductor	1	2	3	4
Near end Z_1(Ω, nH, pF)	(27.4, 2.5, 0)	(1.6×10^3, 0, 1.3)	(6, 0, 0)	(1.6×10^3, 214, 0)
Far end Z_2(Ω, nH, pF)	(7.5, 0, 131)	(1.2×10^3, 303, 0)	(0.49, 0, 0)	(14, 0, 1.2×10^3)

Table 5. Central coordinate of each conductor of the reduced shielding cable bundle (unit: mm).

Conductor	1	2	3	4
Conductor radius	1.5	1.6	2.4	2.5
Central distance	1.5	2	4.2	4
(x,y)	(0, 1.5)	(1, −1.73)	(3.99, 1.3)	(−3.46, −2)

3.2. Comparing results

The induced CM current at the near and far ends of each cable in frequency domain are calculated by using CST Cable Studio. Based on the co-simulation technique, the adopted numerical approach uses the TLM technique to analyze the electric field around the conductors and then use AC result solver to compute the coupling to terminal loads. These computations correspond to the case of a plane wave illumination with a 1 V/m magnitude, the propagation direction 45° with respect

to the reference conducting ground plane and the electric field direction parallel to the conductor. Figures 6–9 illustrate the comparison between the CM currents obtained at the ends of the complete cable bundle and the reduced cable bundle.

Using the feature selective validation (FSV) technique, it provides a way to validate computational electro magnetics (CEM) and predict the assessment of EMC data.[25,26] The FSV technique is used to evaluate the results between the complete model and the simplified model. The FSV technique shows a measure of the "quality" of the correlation between the two sets of data according to specific criteria. Among those measure indicators, we mainly focus on the total amplitude difference measure (ADM_{tot}), the total feature difference measure (FDM_{tot}), and the total global difference measure (GDM_{tot}). These are available as numerical values and can be converted into a natural language descriptor on a six-level scale: excellent (0–0.1), very good (0.1–0.2), good (0.2–0.4), fair (0.4–0.8), poor (0.8–1.6), and very poor (> 1.6).

The FSV evaluation results of Figs. 6–9 are listed in Table 6. From the visual evaluation, it is obviously found that the agreement between the reduced and complete model results is still satisfactory. Thus, it is demonstrated that the proposed simplification technique can be successfully used to model the CM currents on braid shielding multiconductor cable bundles.

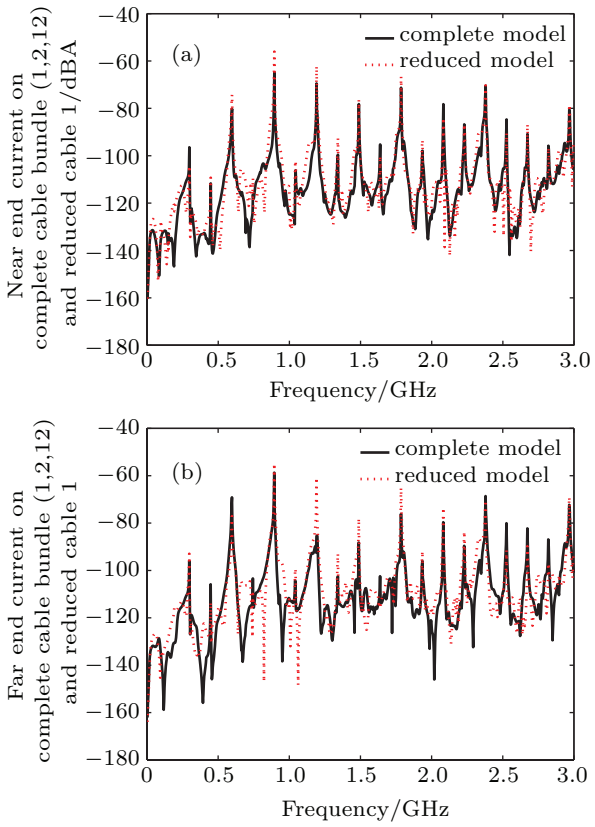


Fig. 6. (color online) Comparison of the CM current in frequency domain on cable 1 between the complete (conductors 1, 2, 12) and reduced cable bundle model: (a) near end; (b) far end.

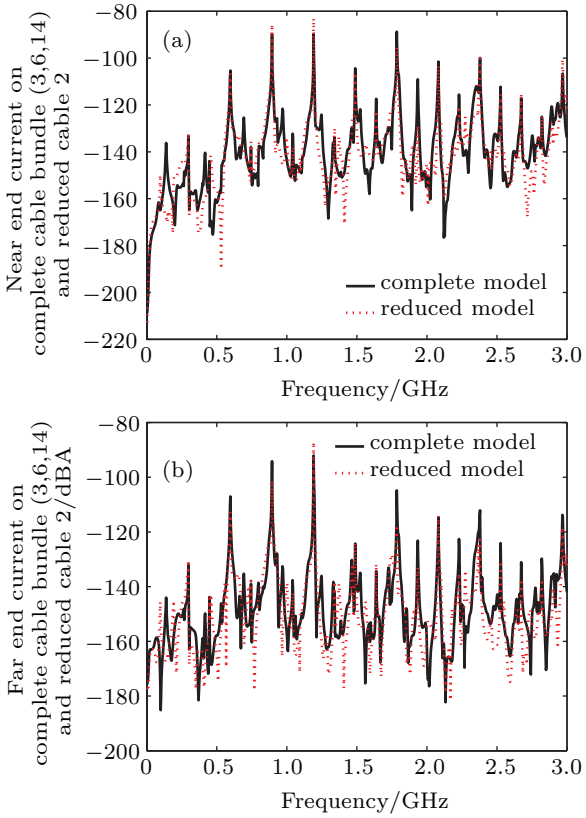


Fig. 7. (color online) Comparison of the CM current in frequency domain on cable 2 between the complete (conductors 3, 6, 14) and reduced cable bundle model: (a) near end; (b) far end.

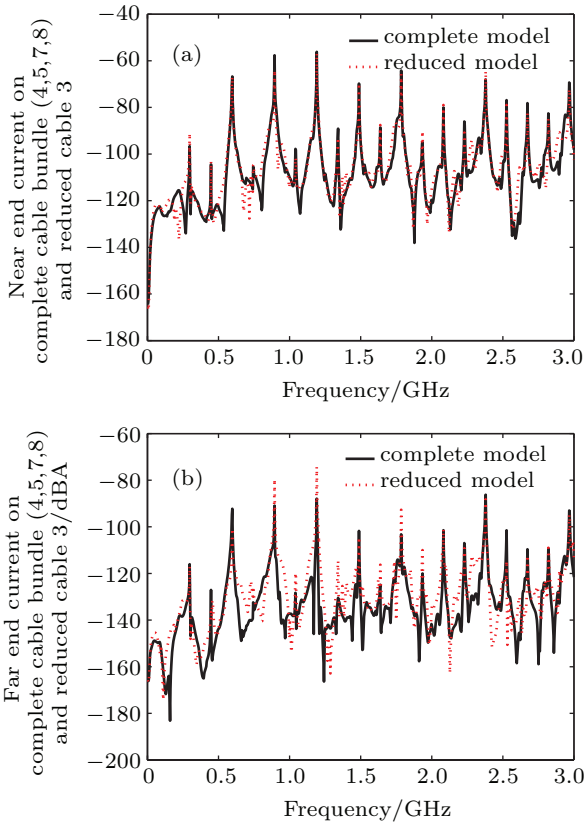


Fig. 8. (color online) Comparison of the CM current in frequency domain on cable 3 between the complete (conductor 4, 5, 7, 8) and reduced cable bundle model: (a) near end; (b) far end.

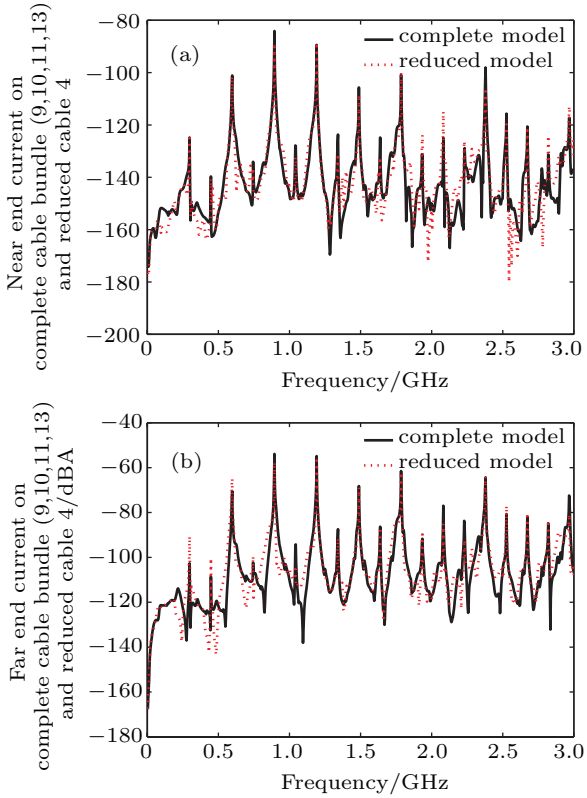


Fig. 9. (color online) Comparison of the CM current in frequency domain on cable 4 between the complete (conductor 9, 10, 11, 13) and reduced cable bundle model: (a) near end; (b) far end.

Table 6. FSV evaluation of results in Figs. 6–9.

Terminals of the TLs	FSV		
	ADM_{tot}	FDM_{tot}	GDM_{tot}
Near end 1	0.239/good	0.351/good	0.465/fair
Far end 1	0.353/good	0.386/good	0.581/fair
Near end 2	0.323/good	0.395/good	0.564/fair
Far end 2	0.356/good	0.428/fair	0.616/good
Near end 3	0.198/very good	0.278/good	0.343/good
Far end 3	0.368/good	0.418/fair	0.612/fair
Near end 4	0.220/good	0.365/good	0.425/fair
Far end 4	0.283/good	0.298/good	0.457/fair

Several reasons are identified to explain the degradation of the agreement at some frequency points. In particular, we suspect the modeling of the cross-section geometry, which is determined by an approximated method. As the terminal loads involve inductance and capacitance, the impedance value is associated with frequency. In this paper, we use the mean value over frequency (0–3 GHz) of the terminal loads of the complete model to represent the equivalent loads.

3.3. Comparison of analysis time

Table 7 shows the computation times for both types of cable bundle models, calculated by CST Cable Studio. The CST simulation configuration is set to satisfy a convergence criterion and all of the computations are completed by a desktop computer with Intel(R) Xeon(R) CPU E3-1231 v3 @3.40 GHz and 32 G RAM under Windows 7. From the table, it is obviously found that the reduced model behaves better in efficiency. Furthermore, it greatly simplifies the modeling process at the expense of certain calculation accuracy.

Table 7. Analysis time of the simplified and complete model.

	Complete cable bundle	Reduced cable bundle
CST	3208 s	1784 s

4. Conclusions

In this paper, we propose a simplification technique to model the EM immunity problem on braid shielding multiconductor cable bundles. In order to conveniently describe the relationship between load impedance and reflection coefficient, a new method of conductors grouping based on the knowledge of Z-Smith chart is presented. Then, a modified six-phase equivalent process is detailed. For the generation of the equivalent cross-section geometrical characteristic parameters, a central distance d and central angle θ are defined and calculated by an approximate method to determine the relative position parameters of the reduced bundle. After that, a coated 14-conductor model is proposed to validate the addressed approach by using the CST.

On the assumption that the CM current response is more critical than the differential-mode response for the EM coupling problems, our technique mainly focuses on the CM currents induced at the terminals of cable bundle. The purpose of the approach is to lower the computation time and simplify the modeling process. The simulation results confirm the possibility to model braid shielding cable bundle. From the analytical process, it can be expected that the bigger.

References

[1] Egot-Lemaire S, Klingler M, Lafon F, Koné L and Baranowski S 2012 *IEEE Trans. Electromag. Compat.* **54** 1222
[2] Ren D, Du P A, Nie B N, Cao Z and Liu W K 2014 *Acta Phys. Sin.* **63** 120701 (in Chinese)
[3] Jiao C Q and Li Y Y 2015 *Chin. Phys. B* **24** 104101
[4] Luo J W, Du P A, Ren D and Nie B L 2015 *Acta Phys. Sin.* **64** 010701 (in Chinese)
[5] Cao Z, Du P A, Nie B L, Ren D and Zhang Q D 2014 *Acta Phys. Sin.* **63** 124102 (in Chinese)
[6] Arianos S, Francavilla M A, Righero M and Vipiana 2014 *IEEE Trans. Electromag. Compat.* **56** 844
[7] Ridel M and Parmantier J P 2014 *International Symposium on Electromagnetic Compatibility*, May 12–16, 2014, Tokyo, Japan, p. 21
[8] Xie H Y, Li Y, Qiao H L and Wang J G 2015 *Chin. Phys. B* **24** 060501
[9] Jobava R G, Gheonjian A L, Hippeli J and Chiqovani G 2014 *IEEE Trans. Electromag. Compat.* **56** 1420
[10] Baum C E, Liu T K and Tesche F M 1978 *Interaction Note* **350** 467547
[11] Wu Z J, Wang L F and Liao C L 2009 *Acta Phys. Sin.* **58** 6146 (in Chinese)
[12] Wan J R, Liu Y P and Zhou H L 2010 *Acta Phys. Sin.* **59** 2948 (in Chinese)
[13] Sun Y X, Zhuo Q K, Jiang Q H and Li Q 2015 *Acta Phys. Sin.* **64** 44102 (in Chinese)

[14] Ferrieres X, Parmantier J P, Bertuol S and Ruddle A R 2004 *IEEE Trans. Electromag. Compat.* **46** 624
[15] Bautista M A E, Francavilla M A, Vipiana F and Vecchi G 2014 *IEEE Trans. Antennas Propag.* **62** 1523
[16] Li G, Hess G, Hoeckele R and Davidson 2015 *IEEE Trans. Electromag. Compat.* **57** 827
[17] Andrieu G, Koné L, Bocquet F and Démoulin B 2008 *IEEE Trans. Electromag. Compat.* **50** 175
[18] Andrieu G, Reineix A, Bunlon X and Parmantier J P 2009 *IEEE Trans. Electromag. Compat.* **51** 108
[19] Li Z, Shao Z J, Ding J and Niu Z Y 2011 *IEEE Trans. Electromag. Compat.* **53** 1040
[20] Li Z, Liu L L, Yan J and Xu A W 2013 *IEEE Trans. Electromag. Compat.* **55** 975
[21] Belkhelfa S, Lefouili M and Drissi K E K 2015 *IEEE Trans. Magn.* **51** 1
[22] Ridel M and Parmantier J P 2012 *Proceedings ESA Workshop on Aerospace EMC*, May 21–23, 2012, Venice, Italy, p. 1
[23] Zheng Y L 2011 *Analysis of Automotive Wiring Harness Equivalent Model and Its Application in Electromagnetic Compatibility Simulation* (Ph. D. Dissertation) (Chongqing: Chongqing University) (in Chinese)
[24] Paul C R 2008 *Analysis of Multiconductor Transmission Lines* (New Jersey: John Wiley & Sons) p. 196
[25] Duffy A P, Martin A J M, Orlandi A and Antonini G 2006 *IEEE Trans. Electromag. Compat.* **48** 449
[26] Orlandi A, Duffy A P, Archambeault B and Antonini G 2006 *IEEE Trans. Electromag. Compat.* **48** 460